Coverage Overlapping Problems in Applications of IEEE 802.15.4 Wireless Sensor Networks

Chao Ma†, Jianhua He†, Hsiao-Hwa Chen‡, and Zuoyin Tang†
†School of Engineering and Applied Science, Aston University, UK.
Email: {mac1, j.he7, z.tang1}@aston.ac.uk
‡Department of Engineering Science, National Cheng Kung University, Taiwan.
Email: hshwchen@ieee.org
Corresponding author: Dr Jianhua He

***Abstract*—IEEE 802.15.4 standard is a relatively new standard designed for low power low data rate wireless sensor networks (WSN), which has a wide range of applications, e.g., environment monitoring, e-health, home and industry automation. In this paper, we investigate the problems of hidden devices in coverage overlapped IEEE 802.15.4 WSNs, which is likely to arise when multiple 802.15.4 WSNs are deployed closely and independently. We consider a typical scenario of two 802.15.4 WSNs with partial coverage overlapping and propose a Markov-chain based analytical model to reveal the performance degradation due to the hidden devices from the coverage overlapping. Impacts of the hidden devices and network sleeping modes on saturated throughput and energy consumption are modeled. The analytic model is verified by simulations, which can provide the insights to network design and planning when multiple 802.15.4 WSNs are deployed closely.**

I. Introduction

A WSN consists of a number of sensor devices deployed over a sensing field. Each device is normally equipped with low-power sensors and capable of sensing information from surrounding environment (e.g., temperature, pressure, etc.). The devices may process acquired data locally, and send the data to one or more collection points, referred to as coordinators [1]. Hence, a WSN can be regarded as a distributed sensing system that may be adequate for many monitoring and controlling applications [2]. WSNs have already been considered for many industrial applications, e.g., smart grid, factory automation [3], distributed process control [4] [5], real-time monitoring of machinery health, detection of liquid/gas leakage, radiation check, etc [6]. As sensor devices normally require low-power consumption, they are difficult to be recharged or replaced. Therefore, low power communication technologies are very important for achieving a long lifetime for WSNs. IEEE 802.15.4 standard [1] has specified physical (PHY) and medium access control (MAC) layers protocols for low-power low data rate wireless personal area networks, which is regarded an excellent candidate for communications among wireless sensors.

Effective performance evaluation is critical for network planning and optimization purposes, especially for WSN applications (such as smart grid) with increasing reliability and data rate requirements. In the literature, there have been a lot of research works on both simulation and theoretical models based performance evaluation of 802.15.4 technology based WSNs. To avoid time-consuming exhaustive simulations, many analytical models were proposed to capture throughput and energy consumption performances of single 802.15.4 network with either saturated or unsaturated traffic. The limited scalability of 802.15.4 MAC protocol was pointed out by Yedavalli *et al.* in [7], which analyzed the performance in terms of throughput and energy consumption. They showed that the 802.15.4 MAC performed poorly when the number of contending devices is high. Misic *et al.* [8] identified a number of potential issues that degrade performance of the MAC protocol, including possible congestions caused by simultaneous attempts of several devices to access wireless medium after an inactive period. Park *et al.* [9] and He *et al.* [10] developed accurate analytical models for 802.15.4 MAC protocol operated in the beacon-enabled mode and star network topology. Energy consumption and throughput performance of 802.15.4 MAC was analyzed in [11]. The problem of uncoordinated coexisting 802.15.4 networks was analyzed in [12] with fully overlapped assumption. However, the partial coverage overlapping problem has not been addressed to the best of our knowledge.

In this paper we attempt to extend our previous analysis [12] on the effectiveness of 802.15.4 MAC for WSNs to the case of multiple WSNs that are closely deployed with partial coverage overlap. A Markov-chain based analytical model is proposed to predict system performance and understand how hidden devices may affect network performance. From the results obtained, it is observed that the hidden devices can lead to a significant system performance drop and reduced network lifetime. For a network with its sleep mode activated, we consider two simple approaches which may be used to enhance network performance, including the reduction in sleep time and overlap ratio g of overlapped proportion in active channel access period of two networks, respectively. Based on the analytical and simulation analysis, we will show that the latter approach can be more effective in alleviating the partial coverage overlapping problem with a small energy cost.

The rest of this paper is organized as follows. Section II briefly introduces channel access algorithm of IEEE 802.15.4 standard. Section III presents the proposed Markov-chain based analytical model for two 802.15.4 networks with partial coverage overlapping. Section IV presents numerical results, followed by the conclusions and future works in Section V.

II. IEEE 802.15.4 STANDARD

Two basic topologies (i.e., star and peer-to-peer) are supported in IEEE 802.15.4 standard. The 802.15.4 networks can work in either beacon-enabled or non-beacon-enabled mode [1]. In this paper we consider a beacon-enabled operation mode, for which a superframe structure is imposed as shown in Fig. 1. As specified, all communications take place in the active period, while devices are allowed to enter a low-power (sleep) mode during the inactive period. The structure of the superframe is characterized by the values of $macBeaconOrder$ (BO) and $macSuperframeOrder$ (SO). BO represents the beacon interval (BI) and SO represents the length of superframe duration (SD). The relationship between these two system variables are shown below.

$$BI = \text{aBaseSuperframeDuration} \times 2^{BO}, \quad (1)$$

$$SD = \text{aBaseSuperframeDuration} \times 2^{SO}, \quad (2)$$

where aBaseSuperframeDuration = 960 symbols and $0 \leq SO \leq BO \leq 14$.

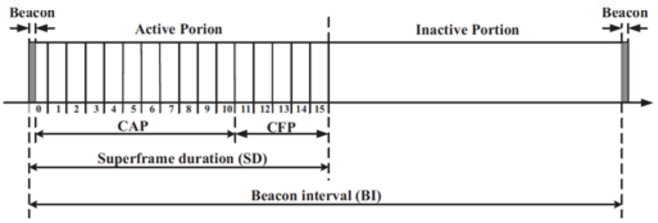

Fig. 1. An example of superframe structure. In this case, the beacon interval (BI) is twice as long as an active superframe duration (SD) and it contains CFP.

The active portion of each BI is composed of two parts: a contention access period (CAP) and optional contention-free period (CFP). We neglect the CFP part in this study, as it is designed for low-latency applications requiring dedicated bandwidth. In the CAP part, communications among devices use slotted CSMA-CA algorithm for contention access. The 802.15.4 slotted CSMA-CA algorithm operates in unit of backoff slot, each having a length of 20 symbols. In the rest of the paper, backoff slot is simply called "slot" unless otherwise specified.

According to the use of acknowledgement (ACK) frame or not for successful reception of a data frame, slotted CSMA-CA algorithm can be operated by MAC layer in two modes: ACK mode if an ACK frame is to be sent and non-ACK mode if an ACK frame is not expected to be sent. In this paper, we will work on the non-ACK mode, but the proposed analytical model can be extended to non-ACK mode. In the specified operations for non-ACK mode, every device in a network maintains three variables for each transmission attempt: NB, W and CW. NB denotes backoff stage, representing backoff times that have been retried while one device is trying to transmit. W denotes backoff window, representing the number of slots that one device needs to back off before CCA. CW represents the contention window length, used to determine how many slots for CCA before transmissions.

Before each device starts a new transmission attempt in the CAP, NB is set to zero and W is set to W_0. The backoff counter chooses a random number from $[0, W_0 - 1]$ and it decreases in every slot without sensing channel until it reaches zero. If two CCAs and frame transmission can be completed in the remaining CAP, the MAC sublayer requests that the PHY perform the first CCA (denoted by CCA1) when backoff counter reaches zero. If channel is idle at CCA1, CW decreases one and the second CCA (denoted by CCA2) is performed after CCA1. If channel is idle for both CCA1 and CCA2, the frame will be transmitted in next slots. If channel is busy in either CCA1 or CCA2, CW resets to two, NB increases by one, and W is doubled but not exceed W_x. If NB is smaller or equal to the allowed number of backoff retries, macMaxCSMABackoffs (denoted by m), the above backoff and CCA processes are repeated. If NB exceeds m, the CSMA-CA algorithm ends. If two CCAs and the frame transmission can not be completed in the remaining CAP, the MAC sublayer waits until the start of the CAP in the next superframe and applies a longer random backoff delay before evaluating whether it can proceed again.

III. SYSTEM MODEL

A. Model Assumption

Let us consider a scenario with two 802.15.4 networks deployed closely and partially overlapped as shown in Fig. 2. These two networks are labelled by NET1 and NET2, with N_1 and N_2 sensor devices in addition to one coordinator in each network, respectively. Each network has a star network topology with one PAN coordinator and operates in a beacon-enabled mode. We set NET1 as the main network and the number of hidden devices from NET2 is $N_{h,2}$. This scenario is practical and may happen when the sensor devices in NET1 and NET2 are far away from each other and they can only hear transmissions from their own networks. Therefore, CCA detection by each sensor device is only affected by transmissions from its own network. In the considered scenario, the coordinators for the networks can detect the transmissions from all sensor devices in their own networks. NET1 coordinator can also hear the transmissions from the hidden devices of NET2. Under this assumption, the transmissions of NET1 may be collided by the data transmissions from hidden devices at the NET1 coordinator.

We also consider the impact of sleeping mode with SO being smaller than BO. The active portion of each BI of hidden devices from NET2 can be overlapped with that of NET1 with a different overlap ratio g as shown in Fig. 3. $g = 1$ means that the CAPs are fully overlapped, and $g = 0$ means there is no overlapping. For simplicity, assuming that the beacons from one network can be correctly received by all sensor devices belonging to that network.

Let us consider only uplink traffic from sensor devices to the coordinators and both networks are operated on the same frequency channel. Each data frame has a fixed length that requires L_1 and L_2 slots for NET1 and NET2, respectively, to transmit over the channel. The data payload in the MAC layer frame is fixed as $L_{d,1}$ and $L_{d,2}$ slots for NET1 and

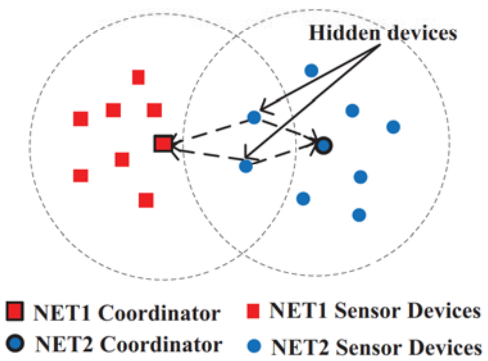

Fig. 2. Communication ranges of two networks are partially overlapped with hidden devices.

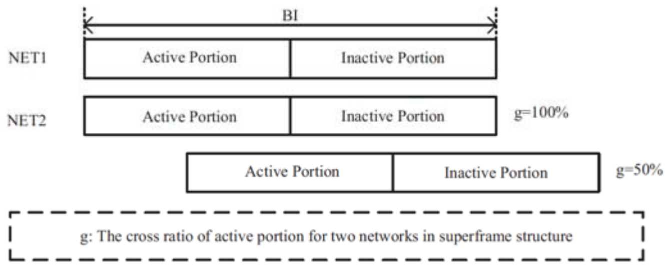

Fig. 3. Illustration of overlap in channel access periods with different overlap ratio g, where g is the ratio of the number of slots in overlapped part to the number of slots in active portion, $0 \leq g \leq 1$.

NET2, respectively, which is transmitted as MAC payload. We assume that the networks have saturated traffic and identical superframe structure. We consider an ideal channel, over which a frame fails if and only if collision happens.

B. Analytical Model

The system performance of NET1 in the CAP can be analyzed separately with two parts according to the overlap ratio g: non-overlapped and overlapped parts. For the non-overlapped part, the system performance of two networks can be analyzed with the existing analytical model for single 802.15.4 network as proposed in [13] due to the fact that there is no interference with each other. According to the idea of performance modeling in [13], the overall channel states sensed by each sensor device of either 802.15.4 network in non-overlapped part can be modeled by a renewal process, which starts with an idle period, followed by a fixed length of L slots (frame transmission).

The slotted CSMA-CA operation of each individual device can be modeled by an Markov chain with finite states. Let $p_{n,k}$ denote the probability that a transmission from sensor devices in network n (n represents network identification, being 1 or 2) other than a tagged sensor device in network n starts after exactly k idle slots since the last transmission, where $k \in [0, W_x+1]$. The transmission probability of a sensor device in a general backoff slot can be calculated with a Markov chain constructed for each device. For the tagged sensor device, its Markov states were introduced by [13], for the sake of space, we only list the definition of the states. Additional specific equations for the states can be found in [13]. For simplicity, we ignore the subscript "1" and "2" that correspond to NET1 and NET2 in the Markov states. In the following derivations, we assume that NET1 and NET2 use the same set of MAC parameters. It is trivial to extend to the cases with different sets of MAC parameters.

1) Busy state, denoted by $B_{i,j,l}$, during which at least one device other than the tagged sensor device transmits the lth part of a frame of L slots, with its backoff stage and backoff counter being i and j, respectively.
2) Backoff state, denoted by $K_{i,j,k}$, during which the tagged sensor device backs off with its backoff counter being j at backoff stage i after k idle slots since the last transmission.
3) Sensing state, denoted by $C_{i,k}$, during which the tagged sensor device performs CCA2 at the ith backoff stage after k idle slots since the last transmission.
4) Initial transmission state, denoted by $X_{i,k}$, during which the tagged sensor device starts to transmit a frame at backoff stage i after k idle slots since the last transmission.
5) Transmission state, denoted by T_l, during which the tagged sensor device transmits the lth part of a frame.

The transmission probability τ_k that the tagged sensor device transmits after exactly k idle slots since the last transmission can be computed by $\tau_k = 0$ for $k \in [0, 1]$, and

$$\tau_k = \sum_{i=0}^{m} \bar{X}_{i,k} \Big/ \sum_{i=0}^{m} \Big[\bar{X}_{i,k} + \bar{C}_{i,k} + \sum_{j=0}^{W_i-1} \bar{K}_{i,j,k}\Big], \quad (3)$$

for $k \in [2, W_x+1]$ [13]. With the above expression derived for transmission probability τ_k ($\tau_{1,k}$ and $\tau_{2,k}$ for NET1 and NET2, respectively), we can calculate channel busy probability p_k ($p_{1,k}$ and $p_{2,k}$ for NET1 and NET2, respectively) with $k \in [0, W_x+1]$ [13] as

$$p_{1,k} = 1 - (1-\tau_{1,k})^{N_1-1}, \quad (4)$$

$$p_{2,k} = 1 - (1-\tau_{2,k})^{N_2-1}. \quad (5)$$

Since the balance equations for all steady state probabilities and expressions for $p_{1,k}$ and $p_{2,k}$, $k \in [0, W_x+1]$, have been derived, the Markov chain for the tagged sensor device can be numerically solved. After the Markov chains are solved, we can calculate the throughput of non-overlapped part S_n^f for individual network [13], or

$$S_n^f = N_n L_{d,n} \sum_{i=0}^{m} \sum_{k=1}^{W_i} C_{n,i,k-1}(1-p_{n,k-1}) \times (1-p_{n,k}), \quad n = 1, 2. \quad (6)$$

In the overlapped part of CAP, the channel access is not affected by channel activities from hidden devices. The only impact of hidden devices on the transmissions in NET1 is the outcomes of frame reception. If a frame transmitted from the tagged sensor device to the coordinator in NET1 does not collide with the frames from the other devices in its own network, it is still subject to collide with frames from hidden devices of NET2. An illustration of the uncoordinated collisions is shown in Fig. 4. The problem that remains to be solved is the calculation of successful frame reception probability, which depends on the transmission probability of hidden devices.

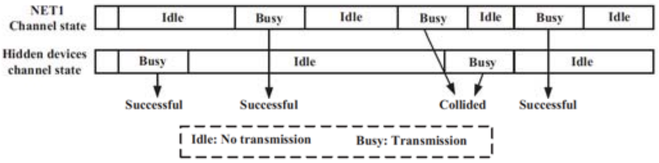

Fig. 4. Example of collision of frames due to coverage overlapping problem.

The transmission probability $\tau_{2,k}$ of NET2 can be computed by equation (3) with the Markov model from [13]. Then, the probability of having exactly k idle slots before one transmission in CAP of NET2 can be derived, which is expressed by $p_{2,idle,k} = 0$ (subscript 2 means NET2) for $k \in [0, 1]$, and for $k \in [2, W_x + 1]$ [12], we have

$$p_{2,idle,k} = \begin{cases} 1 - \left(1 - \tau_{2,k}\right)^{N_2}, & k = 2 \\ \left(1-(1-\tau_{2,k})^{N_2}\right) \\ \times \prod_{z=2}^{k-1} \left(1-\tau_{2,z}\right)^{N_2}, & k \in [3, W_x + 1] \end{cases} \tag{7}$$

The number of hidden devices in NET2 which affect the performance of NET1 is $N_{h,2}$, where $0 \leq N_{h,2} \leq N_2$. $N_{h,2} = 0$ means there is no hidden device within NET1 communication range. For the case of having k idle slots before one transmission in NET2, there is a probability $p_{2,hidle,k}$ (subscript 2 means NET2) that at least one hidden device in NET2 transmits immediately after this k idle slots. For example, in case of $k = 2$, we have

$$p_{2,hidle,2} = \sum_{u=1}^{N_2} \left(C_{N_2}^u - C_{N_2-N_{h,2}}^u\right) \tau_{2,2}^u \left(1 - \tau_{2,2}\right)^{N_2-u}, \tag{8}$$

where $u \in [1, N_2]$ is the number of sensor devices transmitting in the same time slot immediately after k idle slots.

When $u > N_2 - N_{h,2}$, the expression $C_{N_2-N_{h,2}}^u$ is not defined. We set an intermediate variable $N_{2,free,h}$ (subscript 2 means NET2) instead of $C_{N_2-N_{h,2}}^u$, and the definition of $N_{2,free,h}$ is

$$N_{2,free,h} = \begin{cases} 0, & u > N_2 - N_{h,2} \\ C_{N_2-N_{h,2}}^u, & u \leq N_2 - N_{h,2} \end{cases} \tag{9}$$

Now, for any k idle slots before one transmission in NET2, we can get the probabilities of at least one hidden device transmitting immediately after k idle slots as

$$p_{2,hidle,k} = \begin{cases} \sum_{u=1}^{N_2} (C_{N_2}^u - N_{2,free,h}) \tau_{2,k}^u (1 - \tau_{2,k})^{N_2-u}, \\ \qquad\qquad k = 2 \\ \sum_{u=1}^{N_2} (C_{N_2}^u - N_{2,free,h}) \tau_{2,k}^u (1 - \tau_{2,k})^{N_2-u} \\ \times \prod_{z=2}^{k-1} (1 - \tau_{2,z})^{N_2}, \qquad k \in [3, W_x + 1] \end{cases} \tag{10}$$

For each transmission from hidden devices in NET2 following exactly k idle slots, we can define another probability $p_{2,suc,k}$ (subscript 2 means NET2) which means that an independent transmission from NET1 is not collided. It is noted that the probability $p_{2,suc,k}$ is larger than zero only if k is larger or equal to the data length L_1 in NET1. An illustration of the collision of frames from NET1 and hidden devices from NET2 is presented in Fig. 5.

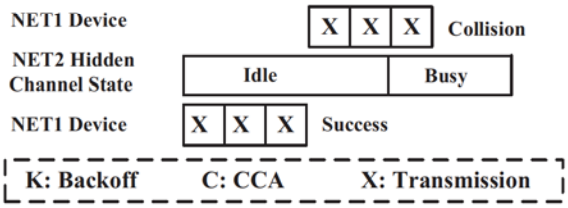

Fig. 5. Illustration of transmissions from NET1 with/without collisions with frames of hidden devices from NET2.

We can calculate $p_{2,suc,k}$ for $k \in [2, W_x + 1]$ by

$$p_{2,suc,k} = \begin{cases} 0, & k < L_1 \\ \frac{k-L_1+1}{k}, & k \geq L_1 \end{cases} \tag{11}$$

The average probability $p_{2,hsuc,avg}$ (subscript 2 means NET2) that a transmission from NET1 does not collide with transmission of hidden devices from NET2 can be calculated by

$$p_{2,hsuc,avg} = \frac{\sum_{k=2}^{W_x+1} k \, p_{2,hidle,k} \, p_{2,suc,k}}{\sum_{k=2}^{W_x+1} (k + L_2) \, p_{2,idle,k}} + \frac{\sum_{k=2}^{W_x+1} (k + L_2)(p_{2,idle,k} - p_{2,hidle,k})}{\sum_{k=2}^{W_x+1} (k + L_2) \, p_{2,idle,k}}, \tag{12}$$

where L_2 is the transmission data length in NET2. The throughput of overlapped part S_1^o in NET1 can be computed by

$$S_1^o = S_1^f p_{2,hsuc,avg}. \tag{13}$$

Finally, the overall throughput S_1 of NET1 with a different overlap ratio g and sleep time can be derived as

$$S_1 = 2^{SO_1 - BO_1} \Big[(1 - g) S_1^f + g S_1^o\Big]. \tag{14}$$

To analyze energy consumption, we use normalized energy consumption (denoted by η_1, where subscript 1 represents NET1), defined in [11] as the average energy consumed to transmit one slot of payload. The energy consumption of transmitting a frame in a slot (denoted by E_t) and performing a CCA (denoted by E_c) in a slot is set to 0.01 mJ and 0.01135 mJ, respectively [11]. η_1 is obtained by

$$\eta_1 = \frac{2^{SO_1 - BO_1} N_1}{S_1} \sum_{i=0}^{m} \Bigg\{ \sum_{l=2}^{L_1} E_c B_{1,i,0,l} + \sum_{k=0}^{W_i+1} \Big[E_c \times (K_{1,i,0,k} + C_{1,i,k}) + L_1 E_t X_{1,i,k} \Big] \Bigg\}. \quad (15)$$

IV. Numerical Results and Evaluation

Let us consider an IEEE 802.15.4 PHY at frequency band 2400-2483.5 MHz with O-OPSK modulation which gives 250 kbps of data rate. With O-OPSK modulation, 4 bits are modulated by each symbol and each slot takes 20 symbols, meaning that at most 3000 slots of data can be transmitted in one second for the PHY. BO for each network is set to six, which means the length of each BI is fixed to 3072 slots (about one second). Then, the length of CAP of each BI is only decided by SOs. There is no inactive portion in BIs when SO is set to six, implying that the networks are working in the non-sleep mode. Typical results are presented with default MAC parameters for both NET1 and NET2, i.e., $W_0 = 2^3$, $W_x = 2^5$, and $m = 4$. The number of hidden devices from NET2 varies to investigate the impact of coverage overlapping problem. The overhead of MAC and PHY headers L_h for both networks is 1.5 slots in total, and the data payload length with header is $L = L_d + L_h$. Each simulation result presented in the figures was obtained from the average of 20 simulations. In each simulation, 10^6 data frames were transmitted.

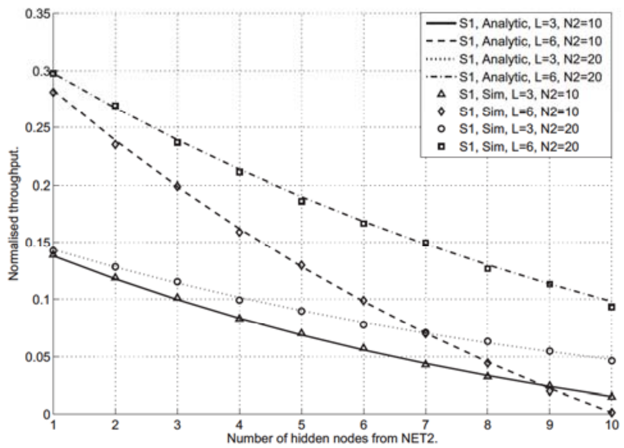

Fig. 6. Normalized throughput S_1 of NET1 with different numbers of hidden devices $N_{h,2}$ from NET2. The number of sensor devices in NET1 is fixed 10, where $L = 3$, $L = 6$, $g = 1$, and $SO = 6$ for each network. The number of sensor devices in NET2 is $N_2 = 10$ and $N_2 = 20$, respectively.

Figure. 6 shows saturated throughput of NET1 as a function of the number of hidden devices from NET2. $SO = 6$ and $g = 1$ indicate that two networks are working in the non-sleep mode with CAPs fully overlapped in each BI. The results in Fig. 6 clearly point out that the more hidden devices the poorer performance the 802.15.4 MAC protocol can achieve. We set the number of sensor devices in NET1 is ten and varied the number of sensor devices in NET2 as 10 and 20, respectively. It is observed that the throughput of NET1 drops quickly with 10 sensor devices in NET2 compared to 20 sensor devices in NET2. This can be explained by the fact that with a larger number of sensor devices in NET2, the transmission probability of the hidden devices will be smaller. Consider the case of 10 sensor devices in NET2. The throughput of NET1 drops to about 0.1 and 0.07 with 3 and 5 hidden devices, respectively, for $L = 3$, showing that each sensor device can deliver about 10 and 7 data messages per second with a message size $L = 3$. With a larger frame length ($L = 6$), the throughput of NET1 drops lower than the case with $L = 3$. In the scenario of 10 sensor devices in NET2, the throughput of NET1 with $L = 6$ becomes lower than the case with $L = 3$ when two networks are nearly fully overlapped. The results presented above show that the impact of hidden devices in the coverage overlapping problem can become more and more serious with the increasing number of overlapping hidden devices. The performance of transmissions with a larger frame length can be effected more severe than a shorter frame length, especially among networks with a relative small number of sensor devices.

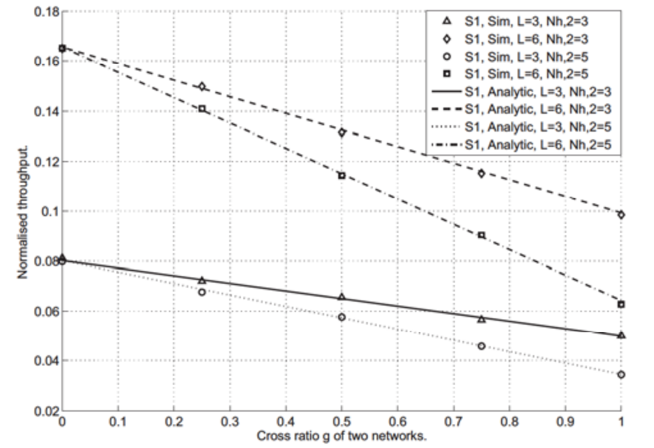

Fig. 7. Normalized throughput S_1 of NET1 with different overlap ratio g. The numbers of sensor devices in NET1 and NET2 are both fixed as 10. The number of hidden devices from NET2 is 3 and 5, respectively, where $L = 3$, $L = 6$, and $SO = 5$ for each network.

We also investigated the effect of overlap ratio g of two networks, while leaving the number of sensor devices $N_1 = N_2 = 10$ and $SO = 5$ for two networks unchanged. The trend is shown in Fig. 7. It is observed that, with an increasing overlap ratio g from 0 to 1, which indicates the situation from no interference to fully overlapped in CAPs among hidden devices from NET2 and sensor devices in NET1, the throughput of NET1 drops linearly. We used $N_1 = N_2 = 10$ and $H_{h,2} = 3, 5$ as examples. It can be proved that the throughput of NET1 drops further with a larger frame length when increasing overlap ratio g, meaning that the larger frame length, the more vulnerable to coverage overlapping problem. It also shows that, without surprise, more hidden devices from NET2 gives a lower throughput of NET1. Consider the case of $L = 6$ with $N_{h,2} = 3$. When there is no interference from hidden devices ($g = 0$), the saturated throughput of NET1 is at most 0.165, which means that at most 82.5 data messages can be successfully transmitted per second and each device can deliver at most 8.25 data messages per second. With an increasing overlap ratio g to 1, the throughput of NET1 drops to about 0.1 and 0.06 for $H_{h,2} = 3$ and 5, respectively, indicating that only about 50 and 30 data messages can be successfully transmitted per second and each device can deliver about 5 and 3 data messages per second, respectively. It is observed that, reducing the overlap ratio g of overlapping networks can significantly improve the performance without sacrificing energy consumption. More importantly, it actually reduces the collision probability of frame transmissions from overlapping networks. Adaptive sleep scheme, which can change the superframe structure to minimize the coverage overlapping problem, needs to be worked out as a future work.

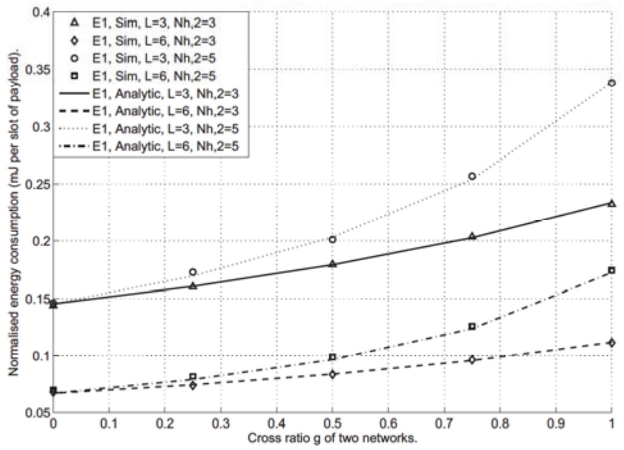

Fig. 8. Normalized energy consumption E_1 of NET1 with different overlap ratio g. The numbers of sensor devices in NET1 and NET2 are both fixed as 10. The number of hidden devices from NET2 is 3 and 5, respectively, where $L = 3$, $L = 6$, and $SO = 5$ for each network.

Finally, Fig. 8 validates the relationship between normalized energy consumption and overlap ratio g in both analytical model and simulations. As expected, the analytical model matches to the simulation results accurately and can predict the energy efficiency very well. The number of sensor devices in both NET1 and NET2 is fixed as 10 and the number of hidden devices from NET2 is 3 and 5, respectively. With an increasing g, the normalized energy consumption increases dramatically. With $L = 6$, consider the case of 5 hidden devices in NET1's communication range. The normalized energy consumption increases from 0.15 mJ per slot of data payload to 0.34 mJ per slot of data payload with an increasing g from 0 to 1, which is more than doubled. It is also proved that, reducing the overlap ratio g of channel access period can efficiently decrease energy consumption, and meanwhile increase throughput.

V. Conclusion

In this paper, we proposed an analytic model to investigate the performance of two IEEE 802.15.4 WSNs which are deployed closely with hidden devices. We have observed a large performance drop in terms of throughput and energy consumption due to the hidden devices. The impact of coverage overlapping problem with various numbers of hidden devices and sleeping mode overlap ratio g was modeled. Simulations demonstrated high accuracy of the proposed analytical model. We also discussed two approaches to improve network performance when hidden devices are present. As WSN applications normally use a long sleep time in practice, reducing the sleeping time by increasing SOs can increase the throughput, but it also increases overall energy consumption at each sensor device. The other efficient way is to reduce the overlap ratio g with the help of adaptive sleeping management schemes and coordinators, which is left as our future work.

Acknowledgement

The work was supported by the UK Engineering and Physical Sciences Research Council (EPSRC) with grant reference number $EP/1010157/1$.

References

[1] IEEE standard for information technology-local and metropolitan area networks-specific requirements-part 15.4: Wireless medium access control (MAC) and physical layer (PHY) specifications for low rate wireless personal area networks (WPANs), IEEE Std 802.15.4-2006 (Revision of IEEE Std 802.15.4-2003), pp. 1 -320, 7 2006.
[2] A. Willig, Recent and emerging topics in wireless industrial communications: A sclection, Industrial Informatics, IEEE Transactions on, vol. 4, no. 2, pp. 102-124, 2008.
[3] D. Miorandi, E. Uhlemann, S. Vitturi, and A. Willig, Guest editorial: Special section on wireless technologies in factory and industrial automation, part I, Industrial Informatics, IEEE Transactions on, vol. 3, no. 2, pp. 95-98, 2007.
[4] M. Lemmon, Q. Ling, and Y. Sun, Overload management in sensor actuator networks used for spatially-distributed control systems, in Proceedings of the 1st international conference on Embedded networked sensor systems. ACM, 2003, pp. 162-170.
[5] B. Sinopoli, C. Sharp, L. Schenato, S. Schaffert, and S. Sastry, Distributed control applications within sensor networks, Proceedings of the IEEE, vol. 91, no. 8, pp. 1235-1246, 2003.
[6] K. Low, W. Win, and M. Er, Wireless sensor networks for industrial environments, in Computational Intelligence for Modeling, Control and Automation, 2005 and International Conference on Intelligent Agents, Web Technologies and Internet Commerce, International Conference on, vol. 2. IEEE, 2005, pp. 271-276.
[7] K. Yedavalli and B. Krishnamachari, Enhancement of the ieee 802.15. 4 MAC protocol for scalable data collection in dense sensor networks, in Modeling and Optimization in Mobile, Ad Hoc, and Wireless Networks and Workshops, 2008. WiOPT 2008. 6th International Symposium on. IEEE, 2008, pp. 152-161.
[8] J. Misic, S. Shafi, and V. Misic, Performance limitations of the MAC layer in 802.15. 4 low rate WPAN, Computer communications, vol. 29, no. 13-14, pp. 2534-2541, 2006.
[9] P. Park, P. Di Marco, P. Soldati, C. Fischione, and K. Johansson, A generalized Markov chain model for effective analysis of slotted ieee 802.15. 4, in Mobile Ad Hoc and Sensor Systems, 2009. MASS09. IEEE 6th International Conference on. IEEE, 2009, pp. 130-139.
[10] J. He, Z. Tang, H. Chen, and Q. Zhang, An accurate and scalable analytical model for IEEE 802.15. 4 slotted CSMA/CA networks, Wireless Communications, IEEE Transactions on, vol. 8, no. 1, pp. 440-448, 2009.
[11] T. Park, T. Kim, J. Choi, S. Choi, and W. Kwon, Throughput and energy consumption analysis of IEEE 802.15. 4 slotted CSMA/CA, Electronics Letters, vol. 41, no. 18, pp. 1017-1019, 2005.
[12] C. Ma, J. He, H. Chen, and Z. Tang, Uncoordinated coexisting IEEE 802.15. 4 nctworks for machinc to machinc communications, Pccr-to-Peer Networking and Applications, pp. 1-11, 2012.
[13] J. He, Z. Tang, H. Chen, and S. Wang, An accurate Markov model for slotted CSMA/CA algorithm in ieee 802.15. 4 networks, Communications Letters, IEEE, vol. 12, no. 6, pp. 420-422, 2008.